Chapter 7

Loopshaping

This chapter presents a graphical technique for designing a controller to achieve robust performance for a plant that is stable and minimum-phase.

7.1 The Basic Technique of Loopshaping

Recall from Section 4.3 that the robust performance problem is to design a proper controller C so that the feedback system for the nominal plant is internally stable and the inequality

$$\| |W_1 S| + |W_2 T| \|_\infty < 1 \tag{7.1}$$

is satisfied. Thus the problem input data are P, W_1, and W_2; a solution of the problem is a controller C achieving robust performance.

We saw in Chapter 6 that the robust performance problem is not always solvable—the tracking objective may be too stringent for the nominal plant and its associated uncertainty model. Unfortunately, constructive (necessary and sufficient) conditions on P, W_1, and W_2 for the robust performance problem to be solvable are unknown.

In this chapter we look at a graphical method that is likely to provide a solution when one exists. The idea is to construct the loop transfer function L to achieve (7.1) approximately, and then to get C via $C = L/P$. The underlying constraints are internal stability of the nominal feedback system and properness of C, so that L is not freely assignable. When P or P^{-1} is not stable, L must contain P's unstable poles and zeros (Theorem 3.2), an awkward constraint. For this reason, we assume in this chapter that P and P^{-1} are both stable.

In terms of W_1, W_2, and L the robust performance inequality is

$$\Gamma(j\omega) := \left| \frac{W_1(j\omega)}{1 + L(j\omega)} \right| + \left| \frac{W_2(j\omega)L(j\omega)}{1 + L(j\omega)} \right| < 1. \tag{7.2}$$

This must hold for all ω. The idea in loopshaping is to get conditions on L for (7.2) to hold, at least approximately. It is convenient to drop the argument $j\omega$.

We are interested in alternative conditions under which (7.2) holds. Recall from Section 6.1 that a necessary condition is

$$\min\{|W_1|, |W_2|\} < 1,$$

so we will assume this throughout. Thus at each frequency, either $|W_1| < 1$ or $|W_2| < 1$. We will consider these two cases separately and derive conditions comparable to (7.2).

We begin by noting the following inequalities, which follow from the definition of Γ:

$$(|W_1| - |W_2|)|S| + |W_2| \le \Gamma \le (|W_1| + |W_2|)|S| + |W_2|, \tag{7.3}$$

$$(|W_2| - |W_1|)|T| + |W_1| \le \Gamma \le (|W_2| + |W_1|)|T| + |W_1|, \tag{7.4}$$

$$\frac{|W_1| + |W_2 L|}{1 + |L|} \le \Gamma \le \frac{|W_1| + |W_2 L|}{|1 - |L||}. \tag{7.5}$$

- Suppose that $|W_2| < 1$. Then from (7.3)

$$\Gamma < 1 \quad \Longleftarrow \quad \frac{|W_1| + |W_2|}{1 - |W_2|}|S| < 1, \tag{7.6}$$

$$\Gamma < 1 \quad \Longrightarrow \quad \frac{|W_1| - |W_2|}{1 - |W_2|}|S| < 1. \tag{7.7}$$

  Or, in terms of L, from (7.5)

$$\Gamma < 1 \quad \Longleftarrow \quad |L| > \frac{|W_1| + 1}{1 - |W_2|}, \tag{7.8}$$

$$\Gamma < 1 \quad \Longrightarrow \quad |L| > \frac{|W_1| - 1}{1 - |W_2|}. \tag{7.9}$$

  When $|W_1| \gg 1$, the conditions on the right-hand sides of (7.6) and (7.7) approach each other, as do those in (7.8) and (7.9), and we may approximate the condition $\Gamma < 1$ by

$$\frac{|W_1|}{1 - |W_2|}|S| < 1 \tag{7.10}$$

  or

$$|L| > \frac{|W_1|}{1 - |W_2|}. \tag{7.11}$$

  Notice that (7.10) is like the nominal performance condition $|W_1 S| < 1$ except that the weight W_1 is increased by dividing it by $1 - |W_2|$: Robust performance is achieved by nominal performance with a larger weight.

- Now suppose that $|W_1| < 1$. We may proceed similarly to obtain from (7.4)

$$\Gamma < 1 \quad \Longleftarrow \quad \frac{|W_2| + |W_1|}{1 - |W_1|}|T| < 1,$$

$$\Gamma < 1 \quad \Longrightarrow \quad \frac{|W_2| - |W_1|}{1 - |W_1|}|T| < 1$$

  or from (7.5)

$$\Gamma < 1 \quad \Longleftarrow \quad |L| < \frac{1 - |W_1|}{|W_2| + 1},$$

$$\Gamma < 1 \quad \Longrightarrow \quad |L| < \frac{1 - |W_1|}{|W_2| - 1}.$$

When $|W_2| \gg 1$, we may approximate the condition $\Gamma < 1$ by

$$\frac{|W_2|}{1-|W_1|}|T| < 1 \tag{7.12}$$

or

$$|L| < \frac{1-|W_1|}{|W_2|}. \tag{7.13}$$

Inequality (7.12) says that robust performance is achieved by robust stability with a larger weight.

The discussion above is summarized as follows:

$\|W_1\| \gg 1 > \|W_2\|$	$\|L\| > \frac{\|W_1\|}{1-\|W_2\|}$
$\|W_1\| < 1 \ll \|W_2\|$	$\|L\| < \frac{1-\|W_1\|}{\|W_2\|}$

For example, the first row says that over frequencies where $|W_1| \gg 1 > |W_2|$ the loopshape should satisfy

$$|L| > \frac{|W_1|}{1-|W_2|}.$$

Let's take the typical situation where $|W_1(j\omega)|$ is a decreasing function of ω and $|W_2(j\omega)|$ is an increasing function of ω. Typically, at low frequency

$$|W_1| > 1 > |W_2|$$

and at high frequency

$$|W_1| < 1 < |W_2|.$$

A loopshaping design goes very roughly like this:

1. Plot two curves on log-log scale, magnitude versus frequency: first, the graph of

$$\frac{|W_1|}{1-|W_2|}$$

over the low-frequency range where $|W_1| > 1 > |W_2|$; second, the graph of

$$\frac{1-|W_1|}{|W_2|}$$

over the high-frequency range where $|W_1| < 1 < |W_2|$.

2. On this plot fit another curve which is going to be the graph of $|L|$: At low frequency let it lie above the first curve and also be $\gg 1$; at high frequency let it lie below the second curve and also be $\ll 1$; at very high frequency let it roll off at least as fast as does $|P|$ (so C is proper); do a smooth transition from low to high frequency, keeping the slope as gentle as possible near crossover, the frequency where the magnitude equals 1 (the reason for this is described below).

3. Get a stable, minimum-phase transfer function L whose Bode magnitude plot is the curve just constructed, normalizing so that $L(0) > 0$.

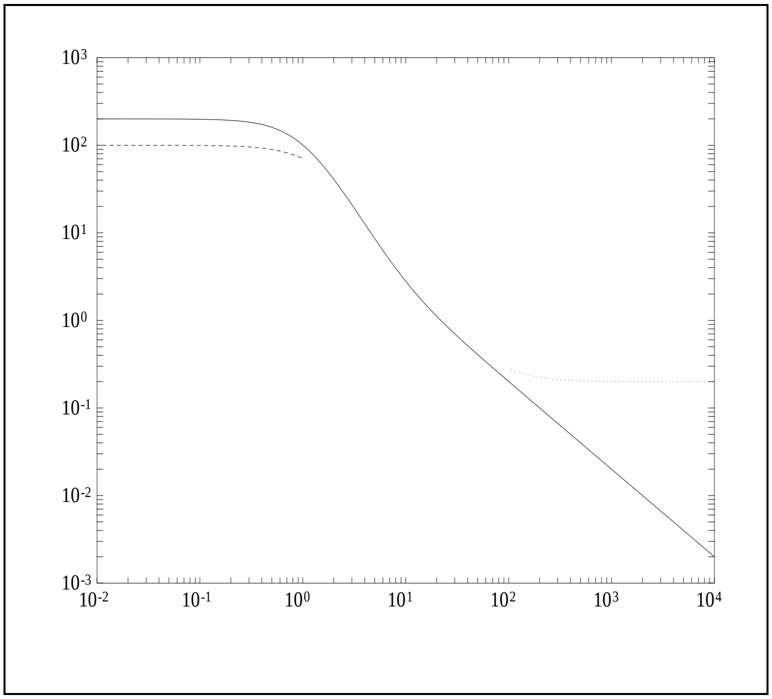

Figure 7.1: Bode plots of $|L|$ (solid), $|W_1|/(1-|W_2|)$ (dash), and $(1-|W_1|)/|W_2|$ (dot).

Typical curves are as in Figure 7.1. Such a curve for $|L|$ will satisfy (7.11) and (7.13), and hence (7.2) at low and high frequencies. But (7.2) will not necessarily hold at intermediate frequencies. Even worse, L may not result in nominal internal stability. If $L(0)>0$ and $|L|$ is as just pictured (i.e., a decreasing function), then the angle of L starts out at zero and decreases (this follows from the phase formula to be derived in the next section). So the Nyquist plot of L starts out on the positive real axis and begins to move clockwise. By the Nyquist criterion, nominal internal stability will hold iff the angle of L at crossover is greater than $180°$ (i.e., crossover occurs in the third or fourth quadrant). But the greater the slope of $|L|$ near crossover, the smaller the angle of L (proved in the next section). So internal instability is unavoidable if $|L|$ drops off too rapidly through crossover, and hence in our loopshaping we must maintain a gentle slope; a rule of thumb is that the magnitude of the slope should not be more than 2. After doing the three steps above we must validate the design by checking that internal stability and (7.2) both hold. If not, we must go back and try again. Loopshaping therefore is a craft requiring experience for mastery.

7.2 The Phase Formula (Optional)

It is a fundamental fact that if L is stable and minimum-phase and normalized so that $L(0)>0$, then its magnitude Bode plot uniquely determines its phase plot. The normalization is necessary, for

$$\frac{1}{s+1} \text{ and } \frac{-1}{s+1}$$

are stable, minimum-phase, and have the same magnitude plot, but they have different phase plots. Our goal in this section is a formula for $\angle L$ in terms of $|L|$.

Assume that L is proper, L and L^{-1} are analytic in $\mathrm{Re}s \geq 0$, and $L(0)>0$. Define $G := \ln L$.

Then

$$\mathrm{Re}G = \ln |L|, \quad \mathrm{Im}G = \angle L,$$

and G has the following three properties:

1. G is analytic in some right half-plane containing the imaginary axis. Instead of a formal proof, one way to see why this is true is to look at the derivative of G:

$$G' = \frac{L'}{L}.$$

   Since L is analytic in the right half-plane, so is L'. Then since L has no zeros in the right half-plane, G' exists at all points in the right half-plane, and hence at points a bit to the left of the imaginary axis.

2. $\mathrm{Re}G(j\omega)$ is an even function of ω and $\mathrm{Im}G(j\omega)$ is an odd function of ω.

3. $s^{-1}G(s)$ tends to zero uniformly on semicircles in the right half-plane as the radius tends to infinity, that is,

$$\lim_{R\to\infty} \sup_{-\pi/2\le\theta\le\pi/2} \left| \frac{G(Re^{j\theta})}{Re^{j\theta}} \right| = 0.$$

Proof Since

$$G(Re^{j\theta}) = \ln |L(Re^{j\theta})| + j\angle L(Re^{j\theta})$$

and $\angle L(Re^{j\theta})$ is bounded as $R \to \infty$, we have

$$\left| \frac{G(Re^{j\theta})}{Re^{j\theta}} \right| \to \frac{|\ln |L(Re^{j\theta})||}{R}.$$

Now L is proper, so for some c and $k \ge 0$,

$$L(s) \approx \frac{c}{s^k} \text{ as } |s| \to \infty.$$

Thus

$$\begin{aligned}\left| \frac{G(Re^{j\theta})}{Re^{j\theta}} \right| &\to \frac{|\ln |c/R^k||}{R} \\ &= \frac{|\ln |c| - k \ln |R||}{R} \\ &\to k\frac{\ln R}{R} \\ &\to 0. \blacksquare\end{aligned}$$

Next, we obtain an expression for the imaginary part of G in terms of its real part.

Lemma 1 *For each frequency* ω_0

$$\mathrm{Im}\ G(j\omega_0) = \frac{2\omega_0}{\pi} \int_0^\infty \frac{\mathrm{Re}G(j\omega) - \mathrm{Re}G(j\omega_0)}{\omega^2 - \omega_0^2} d\omega.$$

Proof Define the function

$$\begin{aligned} F(s) &:= \frac{G(s) - \mathrm{Re}G(j\omega_0)}{s - j\omega_0} - \frac{G(s) - \mathrm{Re}G(j\omega_0)}{s + j\omega_0} \\ &= 2j\omega_0 \frac{G(s) - \mathrm{Re}G(j\omega_0)}{s^2 + \omega_0^2}. \end{aligned} \tag{7.14}$$

Then F is analytic in the right half-plane and on the imaginary axis, except for poles at $\pm j\omega_0$. Bring in the usual Nyquist contour: Go up the imaginary axis, indenting to the right at the points $-j\omega_0$ and $j\omega_0$ along semicircles of radius r, then close the contour by a large semicircle of radius R in the right half-plane. The integral of F around this contour equals zero (Cauchy's theorem). This integral equals the sum of six separate integrals corresponding to the three intervals on the imaginary axis, the two smaller semicircles, and the larger semicircle. Let I_1 denote the sum of the three integrals along the intervals on the imaginary axis, I_2 the integral around the lower small semicircle, I_3 around the upper small semicircle, and I_4 around the large semicircle. We show that

$$\lim_{R\to\infty, r\to 0} I_1 = 2\omega_0 \int_{-\infty}^{\infty} \frac{\mathrm{Re}G(j\omega) - \mathrm{Re}G(j\omega_0)}{\omega^2 - \omega_0^2} d\omega, \tag{7.15}$$

$$\lim_{r\to 0} I_2 = -\pi \mathrm{Im}\ G(j\omega_0), \tag{7.16}$$

$$\lim_{r\to 0} I_3 = -\pi \mathrm{Im}\ G(j\omega_0), \tag{7.17}$$

$$\lim_{R\to\infty} I_4 = 0. \tag{7.18}$$

The lemma follows immediately from these four equations and the fact that $\mathrm{Re}G(j\omega)$ is even.

First,

$$I_1 = \int jF(j\omega)d\omega,$$

where the integral is over the set

$$[-R, -\omega_0 - r] \cup [-\omega_0 + r, \omega_0 - r] \cup [\omega_0 + r, R]. \tag{7.19}$$

As $R \to \infty$ and $r \to 0$, this set becomes the interval $(-\infty, \infty)$. Also, from (7.14)

$$jF(j\omega) = 2\omega_0 \frac{G(j\omega) - \mathrm{Re}G(j\omega_0)}{\omega^2 - \omega_0^2}.$$

Since

$$\frac{\mathrm{Im}\ G(j\omega)}{\omega^2 - \omega_0^2}$$

is an odd function, its integral over set (7.19) equals zero, and we therefore get (7.15).

Second,

$$\begin{aligned} I_2 &= \int_{-\pi/2}^{\pi/2} \frac{G(-j\omega_0 + re^{j\theta}) - \mathrm{Re}G(j\omega_0)}{-j\omega_0 + re^{j\theta} - j\omega_0} jre^{j\theta} d\theta \\ &\quad - \int_{-\pi/2}^{\pi/2} \frac{G(-j\omega_0 + re^{j\theta}) - \mathrm{Re}G(j\omega_0)}{-j\omega_0 + re^{j\theta} + j\omega_0} jre^{j\theta} d\theta. \end{aligned}$$

As $r \to 0$, the first integral tends to 0 while the second tends to

$$[G(-j\omega_0) - \mathrm{Re}G(j\omega_0)]j \int_{-\pi/2}^{\pi/2} d\theta = \pi \mathrm{Im}\ G(j\omega_0).$$

This proves (7.16). Verification of (7.17) is similar.

Finally,

$$I_4 = -\int_{-\pi/2}^{\pi/2} F(Re^{j\theta}) jRe^{j\theta} d\theta,$$

so

$$|I_4| \leq \sup_{-\frac{\pi}{2} \leq \theta \leq \frac{\pi}{2}} \left| \frac{2\omega_0 [G(Re^{j\theta}) - \mathrm{Re}G(j\omega_0)]}{(Re^{j\theta})^2 + \omega_0^2} \right| R\pi.$$

Thus

$$|I_4| \to \text{(const)} \sup_{\theta} \frac{|G(Re^{j\theta})|}{R} \to 0.$$

This proves (7.18). ■

Rewriting the formula in the lemma in terms of L we get

$$\angle L(j\omega_0) = \frac{2\omega_0}{\pi} \int_0^\infty \frac{\ln|L(j\omega)| - \ln|L(j\omega_0)|}{\omega^2 - \omega_0^2} d\omega. \tag{7.20}$$

This is now manipulated to get the phase formula.

Theorem 1 *For every frequency* ω_0

$$\angle L(j\omega_0) = \frac{1}{\pi} \int_{-\infty}^{\infty} \frac{d \ln|L|}{d\nu} \ln\coth\frac{|\nu|}{2} d\nu,$$

where the integration variable $\nu = \ln(\omega/\omega_0)$.

Proof Change variables of integration in (7.20) to get

$$\angle L(j\omega_0) = \frac{1}{\pi} \int_{-\infty}^{\infty} \frac{\ln|L| - \ln|L(j\omega_0)|}{\sinh\nu} d\nu.$$

Note that in this integral $\ln|L|$ is really $\ln|L(j\omega_0 e^\nu)|$ considered as a function of ν. Now integrate by parts, from $-\infty$ to 0 and from 0 to ∞:

$$\begin{aligned} \angle L(j\omega_0) \quad = \quad & -\frac{1}{\pi}\left[(\ln|L| - \ln|L(j\omega_0)|)\ln\coth\frac{\nu}{2}\right]_0^\infty \\ & +\frac{1}{\pi}\int_0^\infty \frac{d\ln|L|}{d\nu}\ln\coth\frac{\nu}{2}d\nu \\ & +\frac{1}{\pi}[(\ln|L| - \ln|L(j\omega_0)|)\ln\coth\frac{-\nu}{2}]_0^\infty \\ & +\frac{1}{\pi}\int_{-\infty}^0 \frac{d\ln|L|}{d\nu}\ln\coth\frac{-\nu}{2}d\nu. \end{aligned}$$

The first and third terms sum to zero. ■

Example Suppose that $\ln|L|$ has constant slope,

$$\frac{d\ln|L|}{d\nu} = -c.$$

Then

$$\angle L(j\omega_0) = -\frac{c}{\pi}\int_{-\infty}^{\infty} \ln\coth\frac{|\nu|}{2} d\nu = -\frac{c\pi}{2};$$

that is, the phase shift is constant at $-90c$ degrees.

In the phase formula, the slope function $d\ln|L|/d\nu$ is weighted by the function

$$\ln\coth\frac{|\nu|}{2} = \ln\left|\frac{\omega+\omega_0}{\omega-\omega_0}\right|.$$

This function is symmetric about $\omega = \omega_0$ (ln scale on the horizontal axis), positive, infinite at $\omega = \omega_0$, increasing from $\omega = 0$ to $\omega = \omega_0$, and decreasing from $\omega = \omega_0$ to $\omega = \infty$. In this way, the values of $d\ln|L|/d\nu$ are more heavily weighted near $\omega = \omega_0$. We conclude, roughly speaking, that the steeper the graph of $|L|$ near the frequency ω_0, the smaller the value of $\angle L$.

7.3 Examples

This section presents three simple examples of loopshaping.

Example 1 In principle the only information we need to know about P right now is its relative degree, degree of denominator minus degree of numerator. This determines the high-frequency slope on its Bode magnitude plot. We have to let L have at least equal relative degree or else C will not be proper. Assume that the relative degree of P equals 1. The actual plant transfer function enters into the picture only at the very end when we get C from L via $C = L/P$.

Take the weighting function W_2 to be

$$W_2(s) = \frac{s+1}{20(0.01s+1)}.$$

See Figure 7.2 for the Bode magnitude plot. Remember (Section 4.2) that $|W_2(j\omega)|$ is an upper bound on the magnitude of the relative plant perturbation at frequency ω. For this example, $|W_2|$ starts at 0.05 and increases monotonically up to 5, crossing 1 at 20 rad/s.

Let the performance objective be to track sinusoidal reference signals over the frequency range from 0 to 1 rad/s. Let's not say at the start what maximum tracking error we will tolerate; rather, let's see what tracking error is incurred for a couple of loopshapes. Ideally, we would take W_1 to have constant magnitude over the frequency range $[0, 1]$ and zero magnitude beyond. Such a magnitude characteristic cannot come from a rational function. Nevertheless, you can check that Theorem 4.2 continues to be valid for such W_1; that is, if the nominal feedback system is internally stable, then

$$\|W_2T\|_\infty < 1 \text{ and } \left\|\frac{W_1S}{1+\Delta W_2T}\right\|_\infty < 1, \quad \forall\Delta$$

iff

$$\||W_1S| + |W_2T|\|_\infty < 1.$$

With this justification, we can take

$$|W_1(j\omega)| = \begin{cases} a, & \text{if } 0 \le \omega \le 1 \\ 0, & \text{else,} \end{cases}$$

where a is as yet unspecified.

Let's first try a first-order, low-pass loop transfer function, that is, of the form

$$L(s) = \frac{b}{cs+1}.$$

It is reasonable to take $c = 1$ so that $|L|$ starts rolling off near the upper end of the operating band $[0, 1]$. We want b as large as possible for good tracking. The largest value of b so that

$$|L| \le \frac{1 - |W_1|}{|W_2|} = \frac{1}{|W_2|}, \qquad \omega \ge 20$$

is 20. So we have

$$L(s) = \frac{20}{s+1}.$$

See Figure 7.2. For this L the nominal feedback system is internally stable.

It remains to check what robust performance level we have achieved. For this we choose the largest value of a so that

$$|L| \ge \frac{a}{1 - |W_2|}, \qquad \omega \le 1.$$

The function

$$\frac{a}{1 - |W_2(j\omega)|}$$

is increasing over the range $[0, 1]$, while $|L(j\omega)|$ is decreasing. So a can be got by solving

$$|L(j1)| = \frac{a}{1 - |W_2(j1)|}.$$

This gives $a = 13.15$.

Now to verify robust performance, graph the function

$$|W_1(j\omega)S(j\omega)| + |W_2(j\omega)T(j\omega)|$$

(Figure 7.2). Its maximum value is about 0.92. Since this is less than 1, robust performance is verified. (We could also have determined as in Section 4.3 the largest a for which the robust performance condition holds.)

Let's recap. For the performance weight

$$|W_1(j\omega)| = \begin{cases} 13.15, & \text{if } 0 \le \omega \le 1 \\ 0, & \text{else,} \end{cases}$$

we can take $L(s) = 20/(s+1)$ to achieve robust performance. The tracking error is then $\le 1/13.15 = 7.6\%$.

Suppose that a 7.6% tracking error is too large. To reduce the error make $|L|$ larger over the frequency range $[0, 1]$. For example, we could try

$$L(s) = \frac{s+10}{s+1}\frac{20}{s+1}.$$

The new factor, $(s + 10)/(s + 1)$, has magnitude nearly 10 over $[0, 1]$ and rolls off to about 1 above 10 rad/s. See Figure 7.3. Again, the nominal feedback system is internally stable. If we take W_1 as before and compute a again we get $a = 93.46$. The robust performance inequality is checked graphically (Figure 7.3). Now the tracking error is $\le 1/93.46 = 1.07\%$.

The problem above is quite easy because $|W_2|$ is small on the operating band $[0, 1]$; the requirements of performance and robust stability are only weakly competitive.

Example 2 This example examines the pitch rate control of an aircraft. The signals are

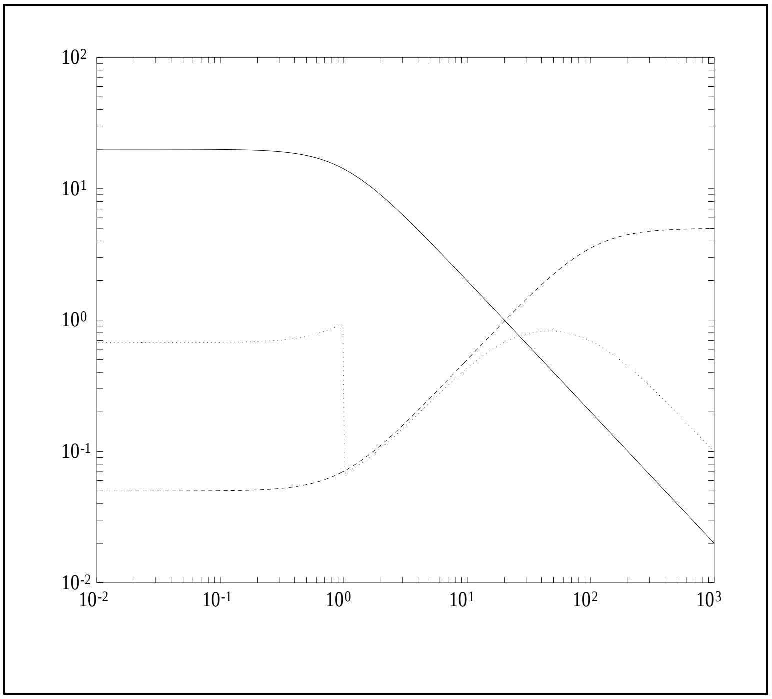

Figure 7.2: Bode plots of $|L|$ (solid), $|W_2|$ (dash), and $|W_1S| + |W_2T|$ (dot).

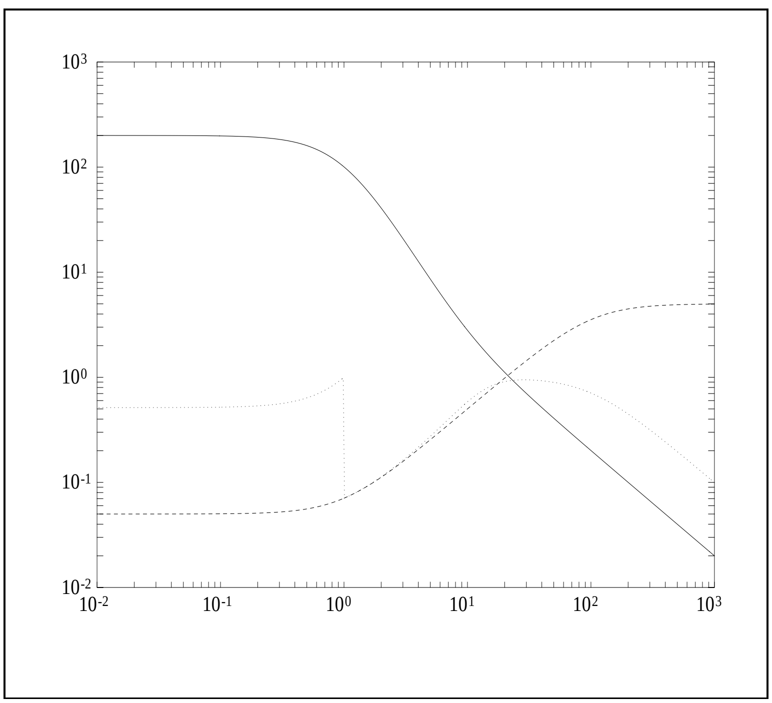

Figure 7.3: Bode plots of $|L|$ (solid), $|W_2|$ (dash), and $|W_1S| + |W_2T|$ (dot).

r pitch rate command (by pilot)

u elevator deflection

y pitch rate of the aircraft

Suppose that the first approximation of the plant is

$$P(s) = \frac{s+1}{s^2 + 2 \times 0.7 \times 5s + 5^2}.$$

This would model the rigid motion of the aircraft (i.e., ignoring bending). The natural frequency is 5 rad/s and the damping ratio 0.7.

Again, rather than specify a performance weight W_1, common practice is to specify a desired loopshape. The simplest decent loop transfer function is

$$L(s) = \frac{\omega_c}{s},$$

where ω_c, a positive constant, is the crossover frequency, where $|L| = 1$. The loopshape $|L(j\omega)|$ versus ω is a straight line (log-log scale) of slope -1.

This is the simplest loopshape having the following features:

1. Good tracking and disturbance rejection (i.e., $|S|$ small) at low frequency.
2. Good robustness (i.e., $|T|$ small) at high frequency.
3. Internal stability.

In principle, the larger ω_c, the better the performance, for then $|S|$ is smaller over a wider frequency range; note that

$$S(s) = \frac{s}{s + \omega_c}.$$

For such L with $\omega_c = 10$, the controller is

$$C(s) = 10\frac{s^2 + 2 \times 0.7 \times s + 5^2}{s(s+1)}.$$

In actuality, there is a limitation on how large ω_c can be because of high-frequency uncertainty: remember that we modeled only the rigid body, whereas the actual aircraft is flexible and has bending modes just as a flexible beam has. Suppose that the first bending mode (the fundamental) is known to be at approximately 45 rad/s. If we included this mode in the transfer function P, there would be a pole in the left half-plane near the point $s = 45j$ on the imaginary axis. This would mean in turn that $|P(j\omega)|$ would be relatively large around $\omega = 45$. For the controller above, the loopshape could then take the form in Figure 7.4. Since the magnitude is greater than 1 at 45 rad/s, the feedback system is potentially unstable, depending on the phase at 45 rad/s.

The typical way to accommodate such uncertainty is to ensure for the nominal plant model that $|L|$ is sufficiently small, starting at the frequency where appreciable uncertainty begins. For example, we might demand that

$$|L(j\omega)| \leq 0.5, \quad \forall \omega \geq 45.$$

(We have implicitly just defined a weight W_2.) The largest value of ω_c satisfying this condition is $\omega_c = 45/2$.

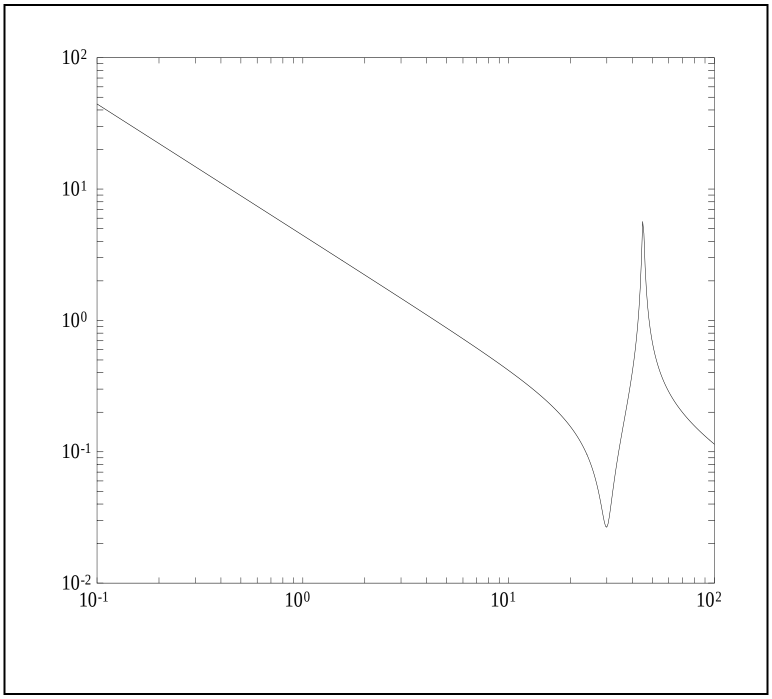

Figure 7.4: Loopshape, Example 2.

Example 3 Consider the plant transfer function

$$P(s) = \frac{s+1}{s^2 + 2 \times 0.7 \times 5s + 5^2} \, \frac{s^2 + 2 \times 0.05 \times 30s + 30^2}{s^2 + 2 \times 0.01 \times 45s + 45^2}.$$

This is an extension of the model of Example 2, with the first bending mode at 45 rad/s included. This mode is very lightly damped, with damping ratio 0.01. This frequency and damping ratio will have associated uncertainty, typically 2 to 3%. Also included in P is an additional pair of lightly damped zeros. The magnitude Bode plot of P is in Figure 7.5. Suppose that the desired loop transfer function is again $L(s) = \omega_c/s$. This would require that $C = L/P$ have the factor

$$s^2 + 2 \times 0.01 \times 45s + 45^2$$

in its numerator, that is, C would be like a notch filter with a very deep notch. But since, as stated above, the numbers 45 and 0.01 are uncertain, a more prudent approach is to have a shallower notch by setting L to be, say,

$$L(s) = \frac{\omega_c}{s} \, \frac{s^2 + 2 \times 0.03 \times 45s + 45^2}{s^2 + 2 \times 0.01 \times 45s + 45^2}.$$

With the same rationale as in Example 2, we now maximize ω_c such that

$$|L(j\omega)| \leq 0.5, \quad \forall \omega \geq 45.$$

This yields $\omega_c \approx 8$ and the loopshape in Figure 7.6. The controller is

$$C(s) = 8 \frac{s^2 + 2 \times 0.7 \times 5s + 5^2}{s(s+1)} \, \frac{s^2 + 2 \times 0.03 \times 45s + 45^2}{s^2 + 2 \times 0.05 \times 30s + 30^2}.$$

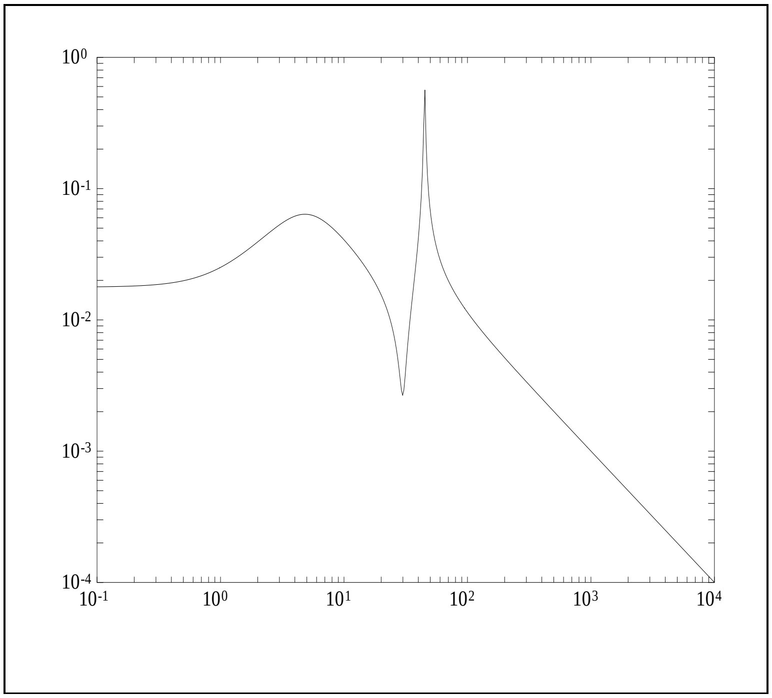

Figure 7.5: Bode plot of $|P|$, Example 3.

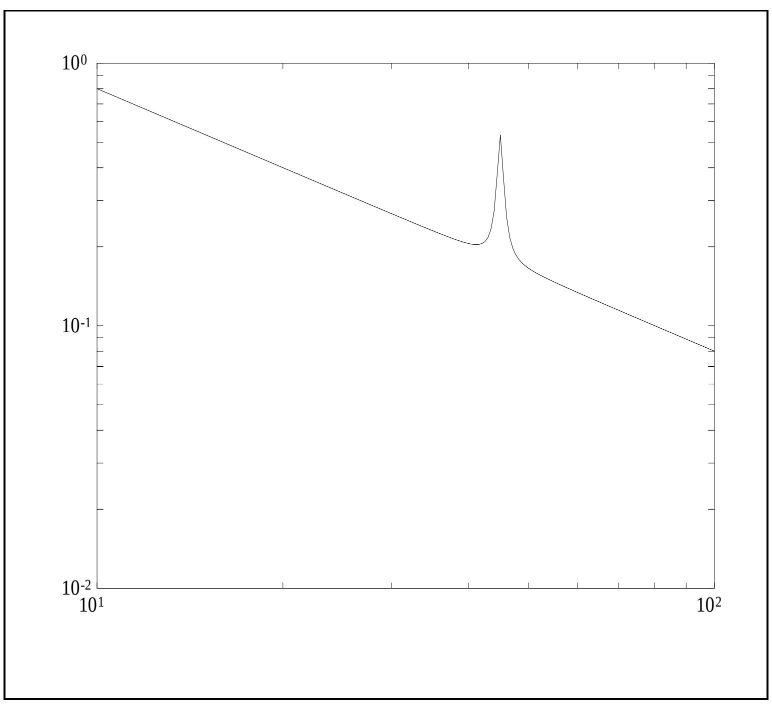

Figure 7.6: Loopshape, Example 3.

Exercises

1. This problem concerns the plant in Example 2 in Section 4.1—the double integrator with an uncertain time delay. Take
$$P(s) = \frac{1}{(s+0.01)^2}.$$
(This is supposed to be a stable approximation to the double integrator.) The time delay was accommodated by embedding the plant in a multiplicative perturbation with weight
$$W_2(s) = \frac{0.1s}{0.05s+1}.$$
To get good tracking over the frequency range $[0,1]$, a typical choice for W_1 would be a Butterworth filter with cutoff of 1 rad/s. To get at most 10% tracking error on the operating band, we would take the gain of the filter to be 10. A third-order such filter is
$$W_1(s) = \frac{10}{s^3+2s^2+2s+1}.$$
For these data, design a controller to achieve robust performance.

2. Repeat the design in Example 1, Section 7.3, but with
$$W_2(s) = \frac{10s+1}{20(0.01s+1)}.$$
This is more difficult because $|W_2|$ is fairly substantial on the operating band. See what performance level a you can achieve.

3. Consider the plant transfer function
$$P(s) = \frac{-s+16}{(s-6)(s+11)}.$$
This is unstable and non-minimum-phase, and loopshaping is consequently difficult for it. But try the loop transfer function
$$L(s) = \frac{\omega_c}{s}\,\frac{-s+16}{16}\,\frac{s+6}{s-6}\,\frac{1}{0.001s+1}.$$
This contains the unstable pole and zero of P, as it must for internal stability; it has relative degree 1, as it must for C to be proper; and it equals approximately $-\omega_c/s$ for low frequency. Compute ω_c to minimize $\|S\|_\infty$. Compute the resulting magnitude Bode plot of S and T.

Notes and References

The technique of loopshaping was developed by Bode for the design of feedback amplifiers (Bode, 1945), and subsequently Bower and Schultheiss (1961) and Horowitz (1963) adapted it for the design of control systems. The latter two references concentrate on particularly simple loopshaping techniques, namely, lead and lag compensation. Loopshaping and the root-locus method are the primary ones used today in practice for single-loop feedback systems. The phase formula is due to Bode. Exercise 3 is based on a simplified analysis of the X-29 experimental airplane (Enns 1986).